

Field effect and magnetoresistance in small bismuth wires*

D. A. Glocker[†] and M. J. Skove

Department of Physics, Clemson University, Clemson, South Carolina 29631

(Received 25 August 1976)

The change in the electrical resistance as a function of applied electrostatic charge, known as the field effect, has been measured in Bi wires ranging in size from 2.6 to 29 μm . These measurements were made at 4.2 K in the presence of applied magnetic fields of varying strengths and directions. The changes in resistance of the samples as a function of applied parallel magnetic field, in fields up to 7×10^5 A/m, have been analyzed as a combination of the bulk longitudinal magnetoresistance and a decrease in the amount of surface scattering. Simultaneous measurements of the field effect in these magnetic fields show, in general, a decrease in the field effect as the surface scattering decreases. When the applied magnetic fields are not parallel to the sample axis the magnetoresistance data indicate increased surface scattering, and an increase in the size of the field effect is also seen. These results are interpreted as suggesting that a major contribution to the field effect in our samples is due to changes in the surface scattering of the intrinsic carriers caused by the added charge. The magnetoresistance data allow us to estimate the specularly coefficient p for two samples to be 0.33 and 0.41, and the change in p with added charge to be $0.1 (\text{C}/\text{m}^2)^{-1}$ and $0.3 (\text{C}/\text{m}^2)^{-1}$.

I. INTRODUCTION

Measurements of the change in the resistance of a sample when the electrostatic charge in the sample is varied (the "field effect") have been made for some time. In the usual experiment, the sample is made one plate of a capacitor and the resistance of the sample measured as a function of the applied charge, which is proportional to the potential difference between the plates. Bismuth shows particularly large changes, although different authors obtain qualitatively different results.¹⁻⁴

In the work presented in this paper we have attempted to avoid some of the possible problems in these measurements by using pure single-crystal Bi and an entirely dc measuring system, which while not as sensitive as ac measuring systems, is less prone to give spurious effects. Since Bi shows a particularly large field effect, we were able to use larger single-crystal samples of Bi despite the relative insensitivity of our apparatus.

The single crystals were fine Bi wires surrounded by glass capillaries ("Taylor wires"). The samples became the inner conductors of small cylindrical capacitors. In order to investigate the possible explanations for the field effect, it was measured as a function of magnetic field applied parallel to the axis of the wire. It has been shown that such a field decreases the scattering of the carriers of the electric current by the surface and we were able to show that this decreased surface scattering leads in general to a lower field effect. In order to evaluate the surface scattering in a semiquantitative manner we have analyzed the pure magnetoresistance in terms of bulk and size contributions, and this in turn enables us to esti-

mate the probability of specular reflection p ; and assuming that the field effect is caused mainly by changes in p , the change in p with added charge.

We will begin by describing the experimental details, and then turn to a discussion of the magnetoresistance results, where we examine the effect of a magnetic field on the surface scattering of the carriers in our samples. We then consider the field-effect results obtained in different magnetic fields, and relate them to the known changes in surface scattering.

II. EXPERIMENTAL TECHNIQUES

The samples used in this experiment were segments of Taylor process⁵ wires, formed by heating and drawing out glass capillaries which had been filled with Bi. During the experiment numerous Taylor wires were made, all by the same basic process. Bi (nominally 99.9999% pure) was forced into a standard Pyrex capillary tube (Corning No. 7740) by melting it in a crucible and drawing it up with an eyedropper bulb. Alternately, the capillary was attached to a vacuum system, a bead of Bi was melted over the mouth of the evacuated capillary, and forced into the capillary by opening the system to the atmosphere or to helium gas at atmospheric pressure. No correlation was found between sample behavior and the use of either of these methods. The inside diameter of a typical Bi-filled capillary at this point was approximately 0.5 mm, and the outside diameter was approximately 5 mm. It was then heated to the softening point of the glass (where the Bi was molten) and rapidly pulled out to form a Taylor wire, with a glass capillary of from 50 to 150 μm in diameter surrounding a Bi wire some ten times smaller

than the glass. Once this was done, a segment could be chosen for use as a sample, or the wire could be zone refined prior to the selection of the sample. Zone refining was done in a small furnace in which two zones, each about 1 cm long, were maintained slightly over the melting point of Bi by Nichrome heating elements. The sample was lowered through the furnace at 7.5 mm/h. Numerous methods were tried in order to make electrical contact to the samples. The one which proved most consistently successful involved a combination of filing and etching through the glass to the Bi. By exposing the Bi at two points on each end of the wire, standard four-probe dc resistance measurements could be made.

Rotating-sample x-ray diffraction patterns were made in order to determine the crystallographic orientation of the samples along their axes. Table I shows the result of these and other measurements. In all, simultaneous magnetic and field-effect measurements were made on 23 samples, but only the final seven were made on a mount which could be oriented with respect to the magnetic field. Since, as we will mention, this was important, only the results for those seven are reported here.

After the data had been taken, the diameter of the glass surrounding each sample, the distance between potential contacts, and the length of the center charging electrode were measured with a calibrated optical microscope. The diameters of the wires were measured by breaking the samples at several places along their lengths, and viewing the cross sections in a scanning electron microscope. The diameter of a given wire typically varied by as

much as $\pm 10\%$ over its length, and the values presented are the averages of the measurements made for each sample. This examination also revealed that the samples were nearly circular in cross section.

In order to measure the change in resistivity due to the field effect, as well as the magnetoresistance, standard four-probe dc resistance measurements were made. Current was supplied to the sample by either a battery-powered constant-current source, which used a feedback-controlled operational amplifier, or by a battery-current source using mercury cells and a large series resistor. The currents, which ranged from 10^{-6} to 10^{-3} A depending on sample resistance, were stable to 1 part in 10^6 . Voltage measurements were made using a Rubicon microvolt potentiometer (model 2768) and a Keithley 147 detector. Figure 1 is a schematic of the charging and measuring circuits. Overall system noise was about $0.1 \mu\text{V}$.

The potential difference between the outer electrode and the sample was supplied by a battery and resistance network. The charging potential could be swept continuously from + 300 to - 300 V. Since very small changes in the voltage across the sample were being measured as a function of large charging voltages, great care was taken to assure that the effect was not due to leakage currents through the sample, or to spurious instrumental effects, by making the following checks:

(i) The field effect was routinely measured at several sample currents, and in all cases the size of the field effect varied linearly with the sample current. At zero current no potential difference along the sample was ever noticeable at any charg-

TABLE I. Summary of sample preparation and characteristics.

Sample No.	Zone refined	Diameter (μm)	Zero-magnetic-field resistivity at		Crystallographic orientation
			4.2 K ($10^{-8} \Omega \text{m}$)	$R_{300}/R_{4.2}$	
<i>a</i> ^a	Yes	11	4.2	34.5	$\langle 111 \rangle$
<i>b</i>	Yes	3.7	6.6	13.5	Polycrystalline
<i>c</i> ^a	Yes	12	14	8.23	High index ^d
<i>d</i> ^a	Yes	12	3.4	47.2	$\langle 111 \rangle$
<i>e</i> ^b	No	6.0	48	2.83	$\langle 11\bar{3} \rangle$
<i>f</i> ^c	Yes	14	6.0	26.7	$\langle 111 \rangle$
<i>g</i> ^a	Yes	10	14	7.64	High index ^d

^a Samples *a* and *d*, and samples *c* and *g*, were each taken from the same original Taylor wire. The Miller indices used refer to the two-atom rhombohedral system.

^b Taken from the same Taylor wire as *b*, but not refined.

^c Taken from the same Taylor wire as *a*, but refined twice.

^d The term "high index" is used to indicate that the samples were single crystals oriented along low-symmetry directions, which had large Miller indices, and their orientation is unknown.

ing voltage.

(ii) The entire charging circuit including the batteries was isolated from ground by greater than $10^{13} \Omega$.

(iii) The resistance from the charging plate to the sample, as measured at the high-voltage inputs to the sample mount while the sample was at 4.2 K, was never less than $10^{13} \Omega$. (The resistance of the glass decreases at higher temperatures.)

(iv) Since the recorder was the only common instrumentation point between the charging and sample circuits, it was removed completely from the circuit on one occasion, and data were taken point by point which agreed completely with the data taken with it in the circuit.

(v) Current sources were used interchangeably without any difference in results.

(vi) During the magnetic measurements, changing the direction of the sample current with respect to the magnetic field from parallel to anti-parallel led to no change in the results.

The charge added to the sample was determined by using the usual capacitance relation

$$q = 2\pi\epsilon_0\epsilon_r V [\ln(r_1/r_2)]^{-1},$$

where q is the charge per unit length of the sample, ϵ_r is the relative dielectric constant of the Pyrex used (given by Corning as 5.1), V is the voltage between the charging lead and the sample, and r_1 and r_2 are the glass and wire radii, respectively. The capacitance of sample c was measured at 77 K using an impedance bridge, and the measured value agreed with that predicted by the above expression.

It was determined after some time that orientation of the samples with respect to the magnetic field was crucial. Therefore, a sample mount was built in which the alignment of the samples could be changed while they were in the magnetic field and at 4.2 K. In order to align the sample parallel to the magnetic field, it was moved at a high field

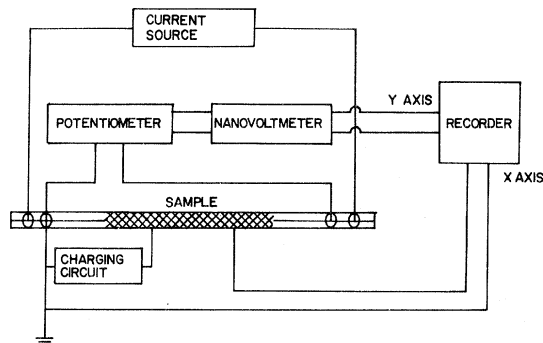


FIG. 1. Schematic illustration of the sample, together with the charging and measuring circuits.

until its resistance was at a minimum with respect to changes in orientation. We estimate that the accuracy of the alignment thus achieved was on the order of $1'$ of arc.

Electrical contact to the sample was made with copper Taylor wires several μm in diameter, which were painted to both the small copper lead wires and to the exposed parts of the sample with silver paint (DuPont No. 7941). The outer charging electrode was made by simply painting the center section of the glass, which surrounded the wire, with silver paint. During the measurements at 4.2 K the sample was immersed in liquid helium. The magnetic fields were produced by a small superconducting coil whose maximum attainable field was 0.9 T.

III. MAGNETORESISTANCE RESULTS

Chambers⁶ has shown that if a magnetic field is applied parallel to the current direction in a small wire, carriers moving in off-axis directions can be made to travel in helices, and thereby avoid collisions with the surface. Consequently, such a magnetic field can lead to a reduction in surface scattering, and therefore a reduction in the resistivity of the sample. Although Chambers's calculations were performed for a simple metal with a spherical Fermi surface and completely diffuse surface scattering, our data reflect this behavior.

Figure 2 summarizes the magnetoresistance re-

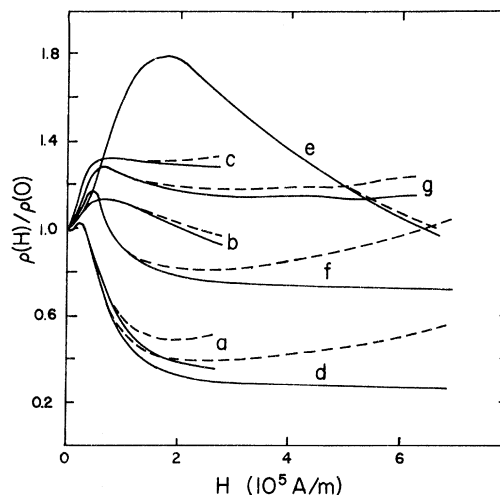


FIG. 2. Summary of magnetoresistance results for all seven samples. The size and residual resistance ratio of the samples are given in Table I. The samples of highest purity show a very nearly complete Chambers decrease in resistance. The solid lines were obtained with the magnetic field parallel to the sample axis to within $1'$ of arc. The dashed lines were obtained with the magnetic field tilted about 1° off the sample axis.

sults with the samples parallel to the magnetic field and with the samples tilted by about 1° with respect to the field. For samples parallel to the field, it is evident that in all but the two smallest wires the magnetoresistances have saturated. This saturation is consistent with Chambers's model, and indicates that at high enough fields the amount of surface scattering has been reduced so much that the resistivity depends mainly on bulk properties. Our interpretation for the other two samples is that the cyclotron radii in these are still large compared to the sample radii at our highest fields, and therefore surface scattering is still important.

In the samples tilted with respect to the field we see no saturation in any case. This is to be expected, since at high fields the carriers are no longer swept away from the surface, but are instead driven into it. As an extreme example of this we remounted sample *d* with its axis tilted by about 23° with respect to the magnetic field (the maximum misalignment allowed by our geometry). The result of this measurement is presented in Fig. 3. We found that after a slight initial decrease, the resistivity rose almost quadratically with respect to the applied field. This qualitative behavior has been predicted by Azbel and Peshanskii⁷ for small samples in transverse magnetic fields. In their model most of the current in such a sample is carried close to the surface, and the specularity of the surface plays an important role in the resistivity.

It should be mentioned that the results presented in Fig. 2 represent the first time the data were taken in each case. On cycling the samples to

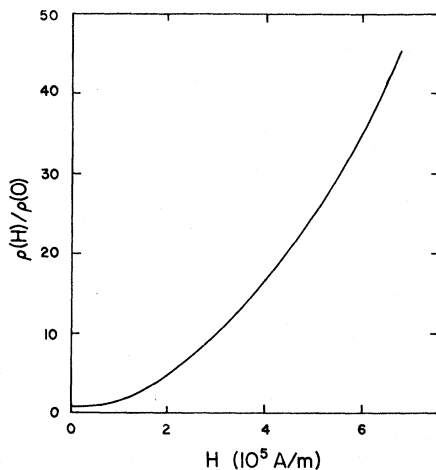


FIG. 3. Magnetoresistance of sample *d* with the magnetic field applied at an angle of 23° with respect to the sample axis.

room temperature and back to 4.2 K, the qualitative behavior was always the same. However, there were quantitative and nonconsistent changes of a few percent in the resistivities at all magnetic fields. Since we interpret our results as due to a combination of bulk and surface effects, plastic deformation of the samples or changes in the Bi-to-glass interface could account for the observed changes in the resistivities.

IV. MAGNETORESISTANCE MODELS

We will now describe the longitudinal magnetoresistance results in terms of a model which combines bulk and surface effects. Because he assumed an isotropic material, the effect described by Chambers does not predict the initial rise in the magnetoresistance of the samples at low fields. Behavior similar to that of our wires has been in small samples of Na, Zn, Bi, and In.^{6,8-10} Olsen¹⁰ suggested that this was a combination of bulk and size effects, but was unable to arrive at theoretical agreement with his results. We have taken an approach very similar to his and have found reasonably good agreement between calculation and experiment.

The bulk magnetoresistance of a metal depends on the ratio of the carrier lifetime to the cyclotron period. This is expressed by Kohler's rule,¹¹

$$\rho_B(H)/\rho_B(0) = 1 + f(H/\rho_B(0)), \quad (1)$$

where $\rho_B(H)$ is the bulk resistivity at the field H , and $\rho_B(0)$ is the bulk resistivity at zero field. If the sample is small, however, the carrier lifetime is increasing as the surface scattering is reduced, and this is reflected in the resistivity. Consequently the physical situation is best described by a modified Kohler's rule

$$\rho'(H)/\rho_s(H) = 1 + f(H/\rho_s(H)), \quad (2)$$

where we have replaced $\rho_B(0)$ with $\rho_s(H)$, the size-dependent magnetoresistivity which depends only on surface scattering, as discussed by Chambers. The sample parameters which appear in $\rho_s(H)$ are the cyclotron radius r_c , the sample radius r , the bulk zero-field resistivity, and the carrier mean free path λ . Since Bi has no single mean free path or cyclotron radius, any theory which uses one value for each is quite simplified, but as we shall see this assumption gives reasonable results. The prime on $\rho'(H)$ in Eq. (2) indicates that it now represents combined bulk and surface effects.

Several authors have measured the bulk longitudinal magnetoresistance of Bi,¹²⁻¹⁴ and for samples with the trigonal symmetry axis parallel to the sample axis the behavior can be written

$$\rho_B(H)/\rho_B(0) = (1 - \{[\rho_B(0)/H]^2 A^{-1} + V^{-1}\}^{-1})^{-1},$$

in which A and V are constants.¹⁵ With this expression, Eq. (2) becomes

$$\rho'(H)/\rho_s(H) = (1 - \{[\rho_s(H)/H]^2 A^{-1} + V^{-1}\}^{-1})^{-1}. \quad (3)$$

With the exception of the cyclotron radius, the choices for A and V fix the other parameters. This is seen by noticing that at saturation, since $\rho_s(H) = \rho_B(0)$, Eq. (3) becomes $\rho'(H \rightarrow \infty) = \rho_B(0)(1 - V)^{-1}$. Therefore, the choice for V together with the measured saturation resistivity determine $\rho_B(0)$. Similarly, the ratio of the measured saturation resistivity to the measured zero-field resistivity determines the value for λ which we used in calculating $\rho_s(H)$. Looking at this experimental ratio we see that

$$[\rho'(H \rightarrow \infty)/\rho_s(0)]_{\text{expt}} = [\rho_B(0)/\rho_s(0)](1 - V)^{-1}.$$

Since $\rho_B(0)/\rho_s(0)$ depends only on the sample radius and the mean free path, an appropriate value for λ could be chosen. We should note that the values for λ chosen this way are probably low since the expression for λ assumes a completely diffuse surface. Using this λ in the model, however, is consistent, even though in Sec. V we will determine it differently. The cyclotron radius we used in the calculations was the largest hole or electron orbit for the case where H was parallel to the trigonal axis. From the known shape of the Fermi surface in Bi,¹⁶ this value was calculated to be $(3.4 \times 10^{-7} \text{ m T})/B$ (where B is the magnetic induction) for the electrons, and was over three times greater than the largest hole orbit.

In short, the adjustable parameters in our model were A and V . We typically chose these values, determined $\rho_B(0)$ and λ , evaluated numerically the analytical expression for $\rho_s(H)$ given by Chambers, and inserted this into Eq. (3) to find $\rho'(H)$ for vari-

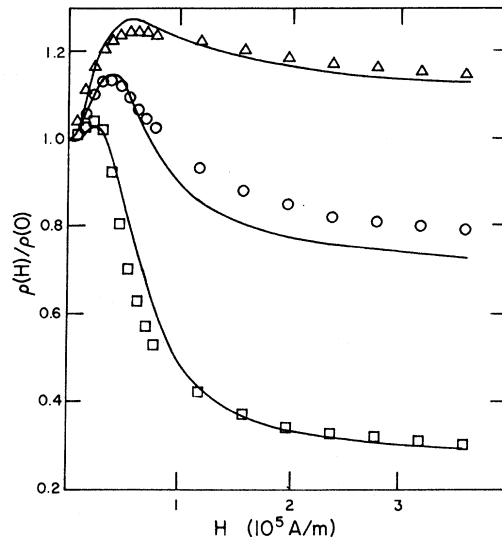


FIG. 4. Comparison of the longitudinal magnetoresistance results for three different samples (solid lines) with the model (points). Δ —fit for sample g with $\rho_B(0) = 1.21 \times 10^{-7} \Omega \text{ m}$, $\lambda = 2.6 \mu \text{ m}$; \circ —fit for sample f with $\rho_B(0) = 2.9 \times 10^{-8} \Omega \text{ m}$, $\lambda = 16 \mu \text{ m}$; \square —fit for sample d with $\rho_B(0) = 4.65 \times 10^{-9} \Omega \text{ m}$, $\lambda = 74 \mu \text{ m}$.

ous values of H . The choices for A and V were then changed to improve the appearance of the fit. Since our object was to see if the experimental features could be duplicated with this model, rather than to produce quantitative results, no curve fitting procedure was used for A and V .

The results of these calculations for three samples, chosen for their spread in characteristics, are presented in Fig. 4. It is clear that the qualitative features of the data are duplicated by the model. Table II compares the parameters used in

TABLE II. Comparison of parameters used in the magnetoresistance model with those found by other investigators, for samples with trigonal symmetry.

	Zitter	Hartman ^b	Gregers-Hansen ^c	Sample d	Sample f
A $10^{-23} \frac{\Omega^2 \text{ m}^2}{\text{A}^2/\text{m}^2}$ ^a	2.02	1.66	2.41	0.08	0.16
V	0.23	0.50	0.33
$\rho_B(0)$ ($10^{-9} \Omega \text{ m}$)	8.0	3.2	5.3	4.7	29
λ^d (10^{-4} m)	...	3.0	...	0.74	0.16
$\rho_B(0)\lambda$ ($10^{-13} \Omega \text{ m}^2$)	...	9.6	...	3.4	4.7

^a In Zitter's notation $A = \rho_{33} \rho_{33,33}$.

^b In Hartman's notation $A = A_{33} \rho_{33}$.

^c In Gregers-Hansen's notation $A = \rho_{33} A_{3333}$.

^d Here λ refers to the mean free path with $H = 0$.

the fits for the two samples with trigonal symmetry with those found in bulk measurements.

We have also tried an alternative model in which we used the value of $\rho_B(H)$ to recalculate λ at each value of the magnetic field, and then used this value of λ in our determination of $\rho_s(H)$. Designating this new value of $\rho_s(H)$ as $\rho'_s(H)$, the second model consisted of calculating

$$\rho'(H) = \rho'_s(H) \left(1 - \left[\frac{\rho_B(0)}{H} \right]^2 A^{-1} + V^{-1} \right)^{-1}.$$

The overall fit given by this was somewhat less good than with the previous model, but the values of the parameters which gave the closest fits were quite similar for both.

The conclusion we reach from these calculations is that our longitudinal magnetoresistance results are consistent with the interpretation that at low magnetic fields the anisotropy of Bi gives rise to bulk changes in the resistivity, and the resistance of our samples increases, while at higher fields a reduction in surface scattering becomes the dominant effect and the resistance decreases. It is also important that this model gives us reasonably reliable values for the bulk resistivities of our samples, and that some of these values are close to those reported for high-quality bulk single crystals.

V. FIELD-EFFECT RESULTS AND DISCUSSION

As a function of applied charge per unit area Q and the applied magnetic field the resistance of our samples typically changed in a fashion which can be represented by the expression

$$R(H, Q) = R(H) + A(H)Q + B(H)Q^2.$$

When written this way, $B(H)$ was usually much smaller than $A(H)$, and depended much less strongly on the magnetic field. In order to determine whether this Q^2 contribution was due to some effect such as the flexing of the sample within the glass during the charging, one wire was etched completely out of the glass in which it was made and was reinserted into a second capillary with some space left between the wire and the glass. The field effect in this specially prepared sample had a much larger than usual Q^2 dependence. Butyl phthalate was then allowed to fill the space, thereby holding the sample stationary at 4.2 K and the Q^2 dependence was reduced considerably. This evidence suggested that $B(H)$ was probably not related to an intrinsic property of our samples.

For the above reasons we chose to characterize the field effect by the expression

$$\delta\rho(H)/\rho(H) \equiv [R(H, +Q) - R(H, -Q)]/R(H, 0).$$

[$R(H, 0)$ is the resistance calculated for that length of sample which was charged.] With this definition the quantity $\delta\rho(H)/\rho(H)$ measures the size of the field effect as a function of applied magnetic field, and is scaled by the appropriate value of the resistance at all magnetic fields.

Figure 5 illustrates typical field-effect results for two of the samples, with the magnetic field both parallel and nonparallel to the current in each case. The system noise expressed in terms of $\delta\rho(H)/\rho(H)$ was about 5×10^{-5} . In all of the results presented here, the field effect was determined for an applied charge density of $\pm 6 \times 10^{-4}$ C/m². Figure 6 presents a summary of the field-effect results for all seven samples, with the current parallel to the magnetic field in each case. These results illustrate that at low magnetic fields where the carrier mobilities (and hence the relative numbers of holes and electrons striking the surface) are changing rapidly as a function of H we see pronounced and rapid changes in the field effect. This suggests that the magnitude, and even the sign,

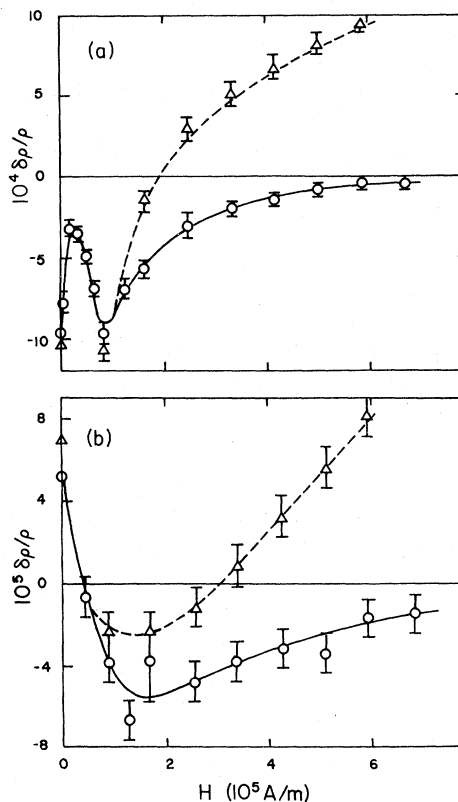


FIG. 5. Field effect as a function of magnetic field for two samples, with H parallel to the sample axes (\circ) and H tilted with respect to the axes by about 1° (Δ). The error bars illustrate the magnitude of the electronic noise and drift in thermal emfs during the measurements. (a) Sample d ; (b) sample g .

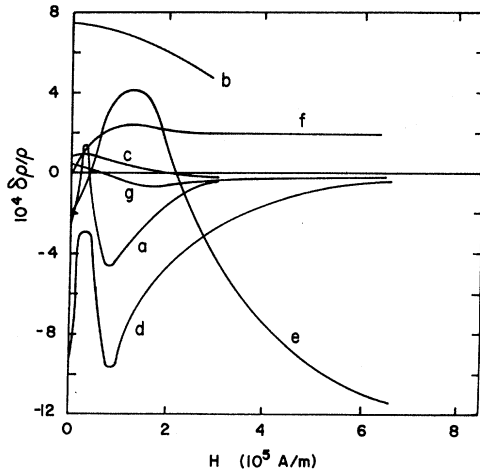


FIG. 6. Summary of the field effects as a function of parallel magnetic fields for all samples. Data for the samples are given in Table I. The individual data points are left off for clarity.

of the field effect in Bi depends strongly on these mobilities.

The second feature which we find interesting in these results is the behavior at high magnetic fields. In the five samples whose magnetoresistances have saturated, the field effects seem to be approaching relatively small, asymptotic values. We interpret this as evidence that a reduction of surface scattering correspondingly reduces the size of the field effect.

This interpretation is supported by the results of the measurements of the field effect made with the samples misaligned with respect to the magnetic field by 1° . Figure 5 illustrates that in this situation the field effects typically no longer saturate, but in fact increase with increasing magnetic field. The most striking example of this behavior is again the data taken for sample 81 with the magnetic field misaligned by 23° . This is presented in Fig. 7. Referring to Fig. 3 and Table I, we see that the actual resistivity of sample *d* at a field of 6×10^5 A/m was 1.4×10^{-6} Ω m, so that the change in resistivity due to the added charge was 3.0×10^{-9} Ω m, or 9% of the zero-field resistivity. It should also be mentioned that, with the exception of sample *e*, the field effects at high nonparallel magnetic fields were always positive.

If we characterize the importance of surface scattering in the resistivities of our samples by the ratio of the mean free path to the sample diameter, an experimental quantity which is proportional to this ratio is $[\rho(H \rightarrow \infty)d]^{-1}$. In Fig. 8 we have plotted the magnitude of the maximum value of $\delta\rho(H)/\rho(H)$ for in a given sample vs $(\rho(H \rightarrow \infty)d)^{-1}$. The trend indicates that the magnitude

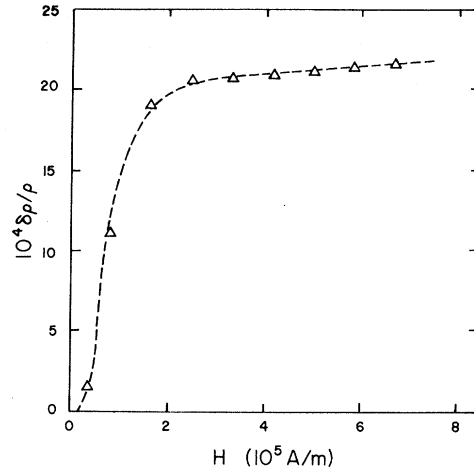


FIG. 7. Field effect as a function of nonparallel magnetic field for sample *d*. The angle between H and the sample axis was 23° .

of the field effect is dependent on the amount of surface scattering which the intrinsic carriers undergo. It is true that other factors such as the specularity coefficient and crystallographic orientation are probably important as well. In addition it is puzzling why the maximum field effect is sometimes positive, and sometimes negative. Nevertheless, the results are suggestive of a field effect which is due in large part to surface scattering in the samples.

On the assumption that the field effect in our samples is due primarily to changes in the surface

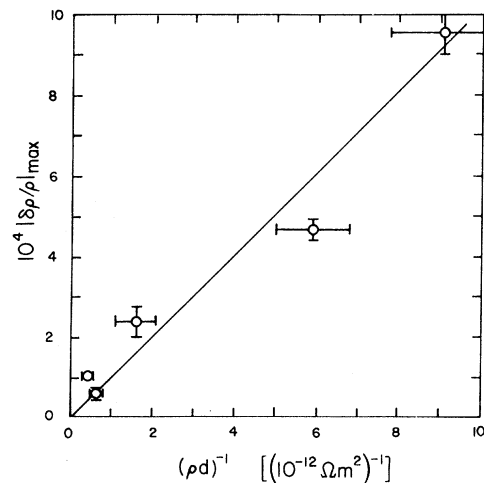


FIG. 8. Magnitude of the maximum field effect in a parallel magnetic field as a function of $(\rho d)^{-1}$. Only the results for those samples whose magnetoresistances have saturated are presented.

TABLE III. Computed values of the bulk resistivity, mean free path, and specularly coefficient for two samples oriented along the trigonal direction.

	$\rho_s(0)$ ($10^{-8} \Omega \text{m}$)	$0.77\rho(H \rightarrow \infty)$ ($10^{-8} \Omega \text{m}$)	λ (10^{-5}m)	d (10^{-5}m)	p
<i>a</i> run 1	4.2	1.1	8.7	1.11	0.35
<i>a</i> run 2	4.4	1.3	7.4	1.11	0.33
<i>d</i> run 1	3.4	0.74	13	1.19	0.41
<i>d</i> run 2	3.7	0.77	12	1.19	0.35

specularity caused by the added charge, we will now calculate p and $\delta p/\delta Q$ for two of our samples. In the case that the mean free path is much greater than the diameter of our samples we can write¹⁷

$$\rho_s(0) = \rho_B(0)(1-p)(1+p)^{-1}(\lambda/d). \quad (4)$$

As mentioned previously $\rho(H \rightarrow \infty) = \rho_B(0)(1-V)^{-1}$. Using Gregers-Hansen's value of $V=0.23$ we can find $\rho_B(0)$ from the measured saturation resistivities, and from Hartman's¹² results we can estimate λ from the expression $\rho_B(0)\lambda = 9.6 \times 10^{-13} \Omega \text{m}^2$. Table III summarizes the values for $\rho_B(0)$, λ , and p determined in this way for samples *a* and *d*. Our values for p agree favorably with that calculated by Friedman⁹ who arrived at $p=0.4$. Further, assuming that p depends on the added charge per unit area, from Eq. (4) above,

$$\delta\rho_s(0)/\rho_s(0) = -[2/(1-p^2)](\delta p/\delta Q)\delta Q.$$

Recalling that Q was $\pm 6 \times 10^{-4} \text{ C/m}^2$ for our samples, and using $\delta\rho(H)/\rho(H)$ at zero magnetic field for samples *a* and *d* we calculate $\delta\rho/\delta Q = 0.1 (\text{C/m}^2)^{-1}$ for *a* and $\delta p/\delta Q = 0.3 (\text{C/m}^2)^{-1}$ for *d*. The only other measurement of this nature of which we are aware was reported recently by Berman and Jurtschke¹⁸ who found a temperature dependence for $\delta p/\delta Q$ in silver films, with a value of $0.14 (\text{C/m}^2)^{-1}$ at 100 K.

The calculations above are intended only as an estimate, and are only possible to make when $\lambda/d \gg 1$ or $\lambda/d \ll 1$, for which cases analytic expressions for $\rho_s(0)$ as a function of p exist. This applies only to our samples *a* and *d*.

VI. CONCLUSION

We have shown that the behavior of the magnetoresistance of our samples when they are placed in high parallel magnetic fields can be explained in terms of diminished surface scattering of the intrinsic carriers. Under these circumstances the

effect of an added charge on the resistance of our samples, when compared to the effect of the same added charge in low or zero magnetic field, is reduced considerably. This strongly suggests that the effect of the added charge is to alter the scattering of the intrinsic carriers at the surface of our samples. This is also consistent with the fact that in magnetic fields not parallel to the sample, where surface scattering is increased as the field strength is increased, the field effect increases with magnetic field. Additional evidence for this model is provided by the fact that the size of the maximum field effect in a given sample is related to the amount of surface scattering in the sample, as measured by $(\rho d)^{-1}$.

The unpredictable changes in the field effect in low magnetic fields may follow from our model as well. It is natural to assume that the effect of an added charge on the scattering of holes and electrons will be different. Therefore, any change in the relative number of holes and electrons striking the surface could cause a change in the magnitude, and perhaps the sign, of the field effect. In low magnetic fields such a change could be caused by two factors; the mean free path of the electrons as a function of magnetic field will change in a different way than that for holes, and the cyclotron radius for holes and electrons is different. It seems possible that a strong dependence of the field effect on the relative number of holes and electrons striking the surface could explain the disagreement among the previously reported results.

ACKNOWLEDGMENTS

The authors would like to thank Dr. James W. Cook, Jr. for his valuable help and suggestions during the course of the experiment. M. J. S. gratefully acknowledges support from the Swiss National Science Foundation during the course of this research.

*Work supported by NSF.

†Present address: Department of Physics, Rochester Institute of Technology, One Lomb Memorial Drive, Rochester, New York 14623.

¹Y. F. Ogrin, V. N. Lutskii, and M. I. Elinson, *Fiz. Tverd. Tela* **9**, 3234 (1967) [*Sov. Phys.-Solid State* **9**, 2547 (1968)].

²L. L. Payne, Ph.D. dissertation (Clemson University, 1974) (unpublished).

³G. Bonfiglioli, E. Coen, and R. Malvano, *Phys. Rev.* **101**, 1281 (1956).

⁴C. Reale, *Phys. Lett.* **A35**, 437 (1971).

⁵J. Strong, *Procedures in Experimental Physics* (Prentice-Hall, New York, 1939).

⁶R. G. Chambers, *Proc. R. Soc. A* **202**, 378 (1950).

⁷M. Y. Azbel and V. G. Peschanskii, *Zh. Eksp. Teor. Fiz.* **49**, 572 (1965) [*Sov. Phys.-JETP* **22**, 399 (1966)].

⁸Yu. P. Gaidukov and N. P. Danilova, *Zh. Eksp. Teor. Fiz.* **64**, 920 (1973) [*Sov. Phys.-JETP* **37**, 467 (1973)].

⁹Allen N. Friedman, *Phys. Rev.* **159**, 553 (1967).

¹⁰J. L. Olsen, *Helv. Phys. Acta* **31**, 713 (1958).

¹¹A. B. Pippard, *The Dynamics of Conduction Electrons* (Gordon and Breach, New York, 1965).

¹²Robert Hartman, *Phys. Rev.* **181**, 1070 (1969).

¹³P. E. Gregers-Hansen, *J. Phys. Chem. Solids* **32**, 1881 (1971).

¹⁴R. N. Zitter, *Phys. Rev.* **127**, 1471 (1962).

¹⁵In Gregers-Hansen's notation $A = \rho_{33}A_{3333}$ and $V = \rho_{33}V_{3333}$.

¹⁶J. E. Aubrey, *J. Phys. Chem. Solids* **19**, 321 (1961).

¹⁷E. H. Sondheimer, *Adv. Phys.* **1**, 1 (1952).

¹⁸A. Berman and H. J. Juretschke, *Phys. Rev. B* **11**, 2903 (1975).